XLI CILAMCE
XLI Ibero-Latin American Congress on Computational Methods in Engineering
16-19 November, 2020 FOZ DO IGUAÇU PARANÁ - BRAZIL

Lumped Element Multibody Modeling Approach for Very Flexible Aircraft

Marko A. Rempel[1], Flávio L. Cardoso-Ribeiro[1], Fernando J. O. Moreira[2]

[1]*Instituto Tecnológico de Aeronáutica*
Praça Marechal Eduardo Gomes, 50, Campus do CTA, São José dos Campos, São Paulo, Brazil
marko.rempel@embraer.com.br, flaviocr@ita.br
[2]*Empresa Brasileira de Aeronáutica S.A.*
Av. Brigadeiro Faria Lima, 2170, São José dos Campos, 12227-901, São Paulo, Brazil
fernando.moreira@embraer.com.br

Abstract. This paper presents a modeling approach using lumped element multibody systems to describe aeroelastic dynamics of aircraft. The model is shown to describe geometric nonlinearities arising from large structural displacements and oscillations such as that of a very flexible wing bending under aerodynamic loads. The presented approach is applied to a Goland's wing to determine the flutter speed resulting from coupling the multibody structure to a quasi-steady aerodynamic model. Flutter velocities are comparable to those obtained using modal representations for structural dynamics. Finally, the modeling appoach is shown to be scalable, parametrized and modular, all of which could make it valuable in iterative environments such as during conceptual design phases of very flexible aircraft.

Keywords: Very Flexible Aircraft, Lumped Elements Multibody System, Aeroelasticity

1 Introduction

Energy efficiency is a decision driver during aircraft design because key performance stats, total life cycle cost and environmental footprint benefit from it. New airframe designs explore weight reduction measures (such as the use of composite materials) and concepts of increased aerodynamic efficiency (such as very high aspect ratio wings) which lead to more flexible aircraft structures.

Increased flexibility reduces structural frequencies, with structural modes approaching flight mechanics modes and demanding use of integrated analyses to capture the resulting behavior. Patil and Hodges [1] demonstrate this for a high-altitude, long-endurance (HALE) flying wing, where the deformed trim shapes also influence flight stability and control. Linearity assumptions loose validity in such cases.

Multibody systems (MBSs) are an alternative to model flexible aircraft. They can describe both flight and structural dynamics and generate good results when coupled to CFD models, as demonstrated in research such as by Krüger and Spieck [2]. Cavagna et al. [3] emphasize that a MBS can model servo-systems, controls, freeplay, friction and nonlinear constitutive laws in a single framework. Furthermore, a MBS can be used to model non-conventional aircraft configurations such as the freely folding wingtip of the AlbatrossONE described by Wilson et al. [4] or tilting rotors on V/STOL aircraft and can handle all kinds of kinematic constraints (such as cargo sliding on rails during airdrops).

Dynamics of structures in a MBS are commonly represented by natural frequencies and mode shapes, relying on geometric linearity assumptions. The present work explores capabilities and limitations of a lumped element approach to describe structural dynamics which can be applicable when modeling slender structures well-described by bending and twisting motion, such as high aspect ratio wings. Capability to cope with geometric nonlinearity is a function of discretization. The approach could prove valuable in iterative environments because it is fully parametric and does not require preprocessing.

The following sections will first assess the quality of a lumped element multibody beam by comparing static deformed shapes and dynamics to benchmarks. Last, the multibody beam model will be coupled to a quasi-steady aerodynamic model to obtain the flutter speed of Goland's wing.

2 Multibody System Description

The multibody model used in this work describes a beam undergoing torsion and bending (both in-plane and out-of-plane). Figure 1 depicts the arrangement of rigid bodies and joints. Additional joints (such as translation joints to model spanwise extension) could be introduced, but system Degrees of Freedom (DoFs) should be restricted to the minimum amount viable since each new joint adds new states to the system.

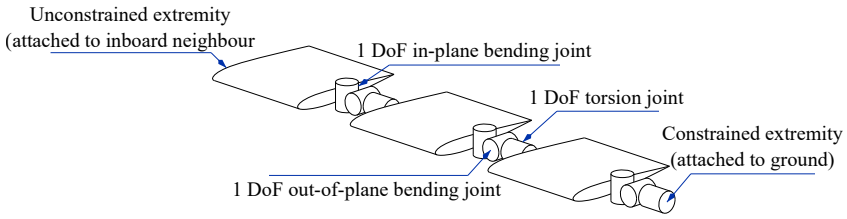

Figure 1. Layout of the multibody wing, built of rigid elements connected by joints.

Challenges will arise if the beam was constrained somewhere else except on its root extremity (such as depicted in Fig. 4) since it is unable to respond to spanwise forces by changes in length. The fixed length also means that an imaginary line conecting adjacent joints is comparable to the neutral axis of real beams, along which no longitudinal strain exists. Figure 1 also assumes the center of twist to be located on the neutral axis.

Rigid bodies have mass and inertia properties. A beam built of n elements thus requires defining n masses and inertias. The Center of Mass is most often not positioned on the neutral axis, which also implies that pure bending or torsion oscillations do not exist: both are coupled by the imbalance.

Finally, structural rigidity and damping are modeled by applying moments to joints. Selecting joint angles as system states is an elegant solution because moments acting on a certain joint become a function of position and speed of the very joint. A different selection of system states would result in distinct expressions for joint moments and would also lead to Equations of Motion (EoMs) of different shape. Symbolic EoMs were obtained using Kane's Method (Kane and Levinson [5]) implementation of SymPy (Meurer et al. [6]) and evaluated numerically with the use of PyDy (Gede et al. [7]).

3 Structural Model Validation

The model's performance was assessed by comparing outputs to results presented by Brown [8]. Demonstrations were split into static and dynamic load cases which gradually increase in complexity. This section tries to demonstrate that large displacement dynamics of slender structures are described adequately by lumped elements.

All beams used by Brown are symmetric, which means that CoMs are positioned along the neutral axis when building the MBS. Torsion and bending consequently uncouple and most examples are 2D (motion is constrained to the *xz*-plane of Fig. 2). In such cases unused joints can be eliminated to reduce computational cost.

3.1 Static Load Cases

Four aspects need to be thought of when formulating any multibody model: kinematics, rigidity, damping and inertia. Static load cases are valuable for validation because influence of damping and inertia are non-existent. Consequently, they allow assessing how good kinematic and rigidity assumptions are.

Figure 2 displays a cantilever beam of constant cross section with a tip force *F(t)* acting on it. The force will be kept constant first, generating a static defomed beam shape. Tip displacement magnitude will increase gradually, resulting in load cases which cannot be solved using geometric linearity assumptions.

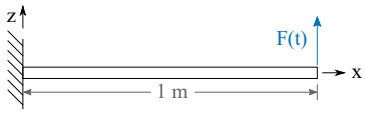

Figure 2. Cantilever beam with concentrated force applied to tip.

The Euler-Bernoulli beam theory taught in engineering textbooks such as Hibbeler [9] formulates displacement as a function of beam loading (*w(x)*, measured in $[N/m]$), where E is the material's Young's modulus, I is the beam's area moment of inertia about the neutral axis (I_y when using the coordinate system of Fig. 2) and v is the resulting displacement:

$$\frac{d^2}{dx^2}\left(EI\frac{d^2v}{dx^2}\right) = w(x). \tag{1}$$

This is an approximation itself best used for slender bodies displaying infinitesimal displacement. Finding the multibody joint stiffness which would result in equal tip displacement as Eq. 1 would lead to a system behaving similarly at small loads and capable of factoring in geometric non-linearity under high loads. Doing so results in the following expression, where n is the number of elements in the MBS and L is the beam's length:

$$k_{joint} = \frac{3EI}{L}\sum_{i=1}^{n}\frac{i^2}{n^2} \quad [Nm/rad]. \tag{2}$$

The expression is applicable to solve any load case as long as EI remains constant and joints are regularly distributed (first joint positioned at the root, same distancing between following joints along the beam). It needs to be reworked if any of the conditions is not met and it could happen that each joint has its own value k_{joint}.

Equation 2 shows that rigidity must increase as joint numbers increase, which is a challenge for dynamic load cases due to high state derivatives, requiring small integration steps. This limits the use of lumped element MBSs to reasonable amounts of bodies. Similarly, introduction of translation joints to model spanwise beam extension would introduce modes of very high natural frequency, further stiffening the EoMs.

Brown's cantilever beam of Fig. 2 has a flexural rigidity $EI = 50\,[Nm^2]$ and length $L = 1\,[m]$. Four multibody beams were built to compare output by varying the number of elements: $n = 3, 5, 10$ and 100. Figure 3 displays beam tip deflection as a function of tip load:

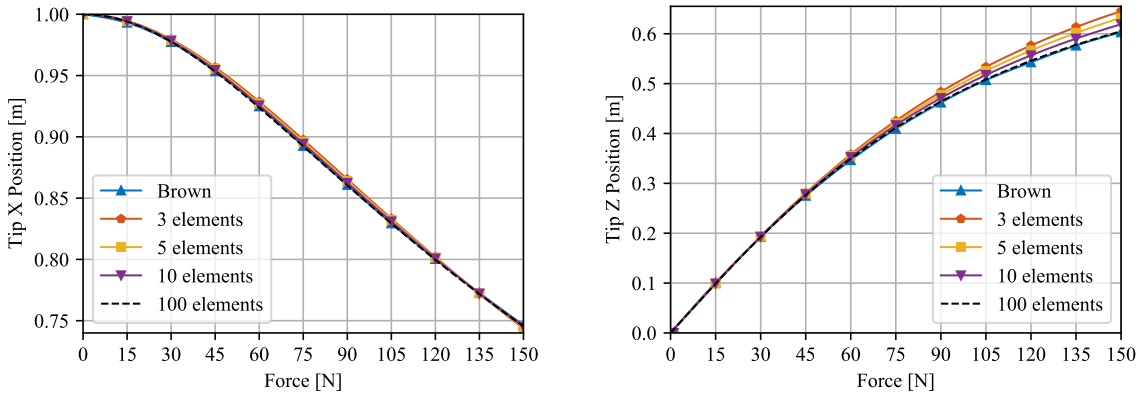

Figure 3. Beam tip position along X and Z axes as a function of vertical load.

Figure 3 shows that all multibody beams generate good results for small loads, but that many rigid elements are necessary to capture geometric non-linearity as loads increase. All beams display the same slope dz_{tip}/dF at $F = 0\,[N]$ because this was the selection criteria of k_{joint}. Furthermore the slope predicted by the Euler-Bernoulli beam theory is close to Brown's slope because the studied beam is slender.

The same methodology to find joint rigidity can be used when solving much more complex structural problems. Figure 4 displays a cantilever beam with an additional constraint: a pin, represented by the black dot, fixes the position of the beam center. The structure is free to rotate around the pin. A possible representation as a MBS could have the beam's center constrained to move on the x-axis, but the center's x-coordinate cannot be constrained without adding degrees of freedom to the system because the beam is made of rigid bodies, unable to

replicate spanwise strain. To compensate for the inaccurate translation constraint being introduced, an additional force of arbitrary magnitude, F_{aux}, was added to the pin, pointing away from the origin.

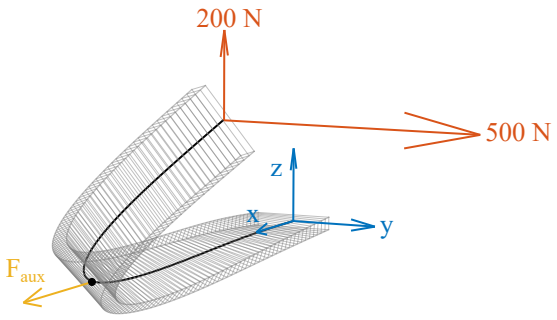

Figure 4. Overconstrained 3D beam with out-of-plane tip force.

The 3D beam has following properties: $EI_y = 39.80\,[Nm^2]$, $EI_z = 1037.2\,[Nm^2]$ and $GJ = 37.31\,[Nm^2]$, where G is the shear modulus of rigidity and J the polar moment of inertia of area. The ratio $I_z/I_y = 26.06$ is not large, which means that in-plane bending of the beam must be accounted for.

Joint rigidity in bending and lead-lag was calculated using Eq. 2 with $n = 100$ elements. Torsional stiffness was chosen such that a torque at the beam tip generates the same angular displacement as it would on a shaft with the same GJ product. Results are presented in Fig. 5 for 3 values of F_{aux}.

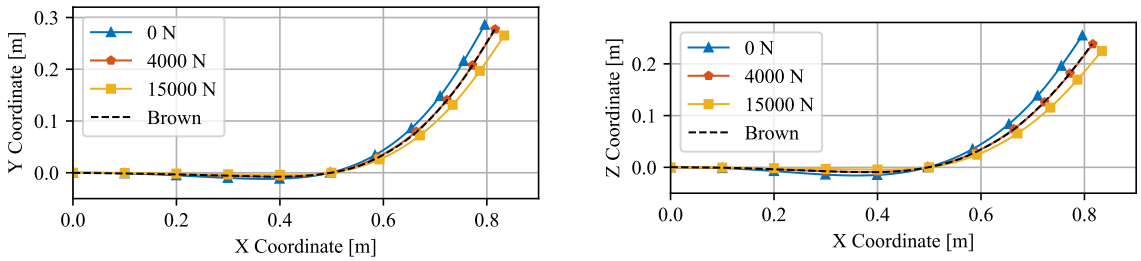

Figure 5. Beam centerline as seen from $-z$ and $+y$ directions.

A multibody beam can handle three-dimensional load cases, but model structure and constraints must be chosen carefully. In this example, where the beam is unable to replicate spanwise strain due to the lack of a translation joint, F_{aux} was calibrated to obtain shapes similar to Brown's.

3.2 Dynamic Response

A possible approach to choose rigidity and kinematic constraints when building a multibody beam was outlined by now. Inertia paramaters (mass, products of inertia, moments of inertia) still need to be selected for each body and should have values consistent with the beam portion they represent. Example: describing a beam of constant density and constant cross section with 5 rigid bodies means that each rigid body should have one fifth of the beam's mass. Structural damping can be added but was considered non-existent.

Modeling efforts presented in this work obtain EoMs which can be integrated to obtain the system's dynamic response but can also be used to extract the system's eigenvalues by linearizing around an equilibrium point. Eigenvalues are a synthesis of the system's dynamic behavior and allow extracting natural frequencies (w_n) and damping (ζ). Dynamic systems with equal eigenvalues display equivalent frequency response.

Han et al. [10] formulate expressions to calculate natural frequencies of transversely vibrating beams using models of varying complexity and demonstrate that for high slenderness ratios (defined by the ratio of length of the beam to the radius of gyration of the cross section) simple models, which do not take into account shear deformation or rotary inertia, output consistent natural frequencies. Feeding the Euler-Bernoulli model with data for the test beam of Fig. 2 ($EI = 50\,[Nm^2]$, $m = 0.2\,[kg]$, $L = 1\,[m]$) outputs $w_n = 55.59\,[rad/s]$ for the first

bending mode, which is in agreement with Brown's result of $w_n = 55.6\,[rad/s]$.

By using the proposed multibody modeling approach, which consists in defining joint rigidity and body inertia by analysis of the structure, w_n is underestimated and will monotonically approach the true value as element numbers increase. Inertia or rigidity parameters could be tuned to achieve closer values for w_n, but this is undesirable. The lumped element approach's main strengths are that it is parametric and does not require preprocessing steps. Tuning parameters to obtain equivalent w_n requires evaluating structural dynamics during preprocessing. The underestimated w_n, on the other hand, can be obtained if basic structural properties such as ρ (material density), E, G and beam geometry are known. Furthermore, the same strategy used to define kinematics, rigidity and inertia can be applied to curved bodies and varying cross-sections with few changes.

Finally, the MBS estimates more than only the first structural mode. A beam of n elements will have n eigenvalues, each representing a mode. To exemplify this, Table 1 lists w_n for the three first modes of an equivalent Euler-Bernoulli beam. Values are compared to output from a multibody beam with 10 elements. As a guideline, w_n prediction quality is poor if a MBS of n elements is used to estimate a mode of order close to n.

Table 1. Natural frequencies of bending modes for the sample cantilever beam.

Structural Mode	w_n $[rad/s]$, Euler-Bernoulli	w_n $[rad/s]$, Multibody ($n = 10$)
1st	55.59	54.30
2nd	348.4	342.1
3rd	975.6	962.1

4 Aeroelastic Coupling Demonstration

The structural model developed so far is able to replicate non-linear geometric displacement and has dynamic modes comparable to the real ones. It can be coupled to an aerodynamic model to generate aeroelastic results. A sample problem was set up to estimate the flutter speed of a uniform cantilever wing studied by Goland [11].

4.1 Aerodynamic Model

Aerodynamic forces were calculated using the Strip Theory approach. Neighbouring sections do not influence each other's lift generation. The spanwise component when decomposing air velocity in the airfoil coordinate system does not generate dynamic pressure. Calculation of lift coefficients assumes $dC_L/d\alpha = 2\pi$ and uses a quasi-steady model developed by Fung [12]:

$$C_L = \frac{dC_L}{d\alpha}\left[\alpha + \frac{1}{U}\frac{dh}{dt} + \frac{1}{U}\left(\frac{3}{4}c - x_0\right)\frac{d\alpha}{dt}\right]. \tag{3}$$

In Fung's formulation α represents the airfoil's angular position, U the freestream velocity and h the vertical position (measured perpendicular to U). Fung also formulates the moment acting on the airfoil about the leading edge:

$$(C_M)_{l.e.} = -\frac{c\pi}{8U}\frac{d\alpha}{dt} - \frac{1}{4}C_L. \tag{4}$$

The second term is a result of the lift force acting on the $1/4$ chord point. The first term is a damping proportional to $\dot{\alpha}$ and stabilizes the system.

4.2 Aeroelastic Results and Discussion

Haddadpour and Firouz-Abadi [13] have calculated Goland's wing flutter speed using different quasi-steady and unsteady aerodynamic models, one of them being Fung's formulation. Modal representations of the 2 first

bending and torsion modes were used to model structural dynamics. Their results provide a reference to assess if the multibody structure generates reasonable flutter speeds when using the same aerodynamic model.

The multibody model built for this example does not have in-plane bending joints to reduce computational cost, which does not mean that resulting dynamics are 2D in nature because combined motion of bending and torsion joints generates complex shapes. This is equivalent to stating that the thickness to chord ratio of the airfoil is so small that resulting structural dynamics are dominated by out-of-plane bending and torsion, which is what Haddadpour and Firouz-Abadi have done by selecting two out-of-plane bending modes and two torsion modes. Dynamic behavior of the aeroelastic system is well described by a root locus, tracking poles as airspeed varies. Figure 6 displays such a root locus for a 6 element multibody wing with one aerodynamic strip per rigid body.

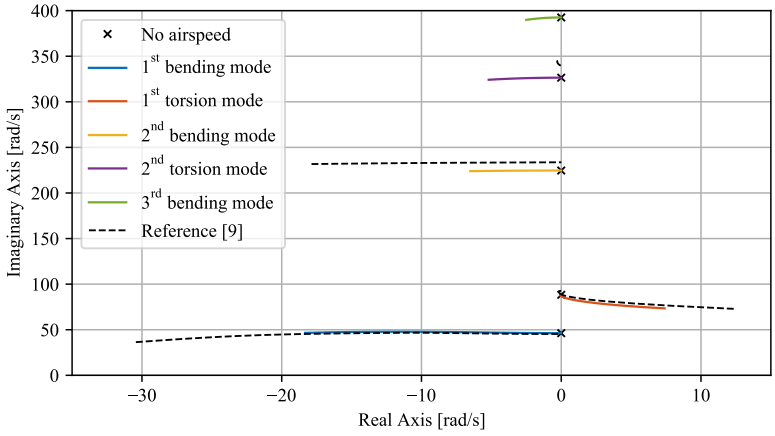

Figure 6. Root locus for the lumped-element multibody wing, airspeed varying from 0 to 100 $[m/s]$.

Pole quantity of the MBS is a function of wing discretization: n elements use $2n$ joints (n for bending and n for torsion), which in turn results in $2n$ pairs of poles. High frequencies describe the structure's higher modes, which in the case of Goland's wing are not the cause of flutter and have been omitted in the plots. Haddadpour and Firouz-Abadi have used 4 modes to represent structural dynamics, resulting in 4 pairs of poles. Figure 6 displays the upper half of the root locus and omits poles with $w_n > 400\,[rad/s]$.

Structural dynamics of the Goland wing in torsion and bending are coupled because center of mass and neutral axis do not coincide. Poles in Fig. 6 nevertheless can be divided into primarily torsion or bending modes. This means that rigidity changes of either torsion or bending joints move one half of the poles considerably more. The pole of second lowest natural frequency is responsible for the flutter phenomena in Fig. 6 because its damping is the first to become negative as air velocity increases. It is the first torsion mode, which means that excitation of the corresponding structural mode results in large torsion of the wing and little bending. Table 2 presents data which can be extracted from the root locus:

Table 2. Flutter of the Goland wing using quasi-steady aerodynamic models.

Structural Model	Flutter Velocity $[m/s]$	Flutter Frequency $[rad/s]$
Modal representation [13]	33.5	93
Multibody (6 elements)	30.8	86.7

The natural frequency of modes in Fig. 6 with no airspeed differ considerably from the reference. An increment in number of elements will monotonically increase frequencies. When using 6 elements, the first bending mode is overestimated while the first torsion mode is underestimated. The reason for this must be understood and constitutes a point for further work. Selection of the neutral axis as the center of twist could be an oversimplification. The underestimated first torsion pole is the probable reason why flutter speeds obtained with the lumped element multibody system are lower than those of Haddadpour and Firouz-Abadi.

System poles can be calculated at any equilibrium point such as the deformed shape of a trimmed, very flexible aircraft. Furthermore the multibody wing captures interplays between bending and torsion dynamics. To exemplify this, the flutter speed of Goland's wing could be increased by $1\ [m/s]$ through a 5% reduction in bending or a 2% increment in torsion joint stiffness. These numbers were obtained without need for preprocessing.

5 Conclusions

A multibody modeling approach is found to adequately describe high-amplitude motion of wing-like structures (high slenderness ratio, small lead-lag motion). By coupling it to a quasi-steady aerodynamic model the multibody system can be used to find flutter speeds comparable to those obtained using mode shape representations. Preliminary results indicate that aeroelastic analyses of slender bodies could benefit from the parametric, modular and scalable nature of lumped parameter multibody systems if geometric nonlinearity must be addressed.

Nevertheless some aspects of the present research must be explored by future work. Most of all, EoM evaluation becomes costly at a low number of rigid bodies, impeding the use of many elements to increase accuracy. When using many elements the modes of high w_n will produce stiff equations, which could mean the system cannot be used for simulation in the time domain. Capabilities to simulate the flight of a flexible aircraft should be demonstrated since the example of this work used a cantilever wing. Last, the differing structural mode frequencies for Goland's wing must be understood. Dynamic benchmark problems where bending and torsion are coupled by mass imbalances must be compared to output from a lumped element MBS.

Acknowledgements. The authors thank the Instituto Tecnológico de Aeronáutica and Embraer for providing the framework which allowed this research to be done.

Authorship statement. The authors hereby confirm that they are the sole liable persons responsible for the authorship of this work, and that all material that has been herein included as part of the present paper is either the property (and authorship) of the authors, or has the permission of the owners to be included here.

References

[1] Patil, M. J. & Hodges, D. H., 2006. Flight dynamics of highly flexible flying wings. *Journal of Aircraft*.
[2] Krüger, W. & Spieck, M., 2004. Aeroelastic effects in multibody dynamics. *Vehicle System Dynamics*, vol. Vol. 41, pp. 383–399.
[3] Cavagna, L., Masarati, P., & Quaranta, G., 2009. Simulation of maneuvering flexible aircraft by coupled multibody/cfd. In *Proc. Multibody Dynamics 2009, ECCOMAS Thematic Conference*, Warsaw, Poland. ECCOMAS.
[4] Wilson, T., Kirk, J., Hobday, J., & Castrichini, A., 2019. Small scale flying demonstration of semi aeroelastic hinged wing tips. In *Proc. International Forum on Aeroelasticity and Structural Dynamics (IFASD, Savannah, GA, 10 - 13 June 2019)*, pp. 1115–1133, Red Hook, NY. Curran Associates, Inc.
[5] Kane, T. R. & Levinson, D. A., 1985. *Dynamics, theory and applications*. McGraw-Hill series in mechanical engineering. McGraw-Hill Book Company.
[6] Meurer, A., Smith, C. P., Paprocki, M., Čertík, O., Kirpichev, S. B., Rocklin, M., Kumar, A., Ivanov, S., Moore, J. K., Singh, S., Rathnayake, T., Vig, S., Granger, B. E., Muller, R. P., Bonazzi, F., Gupta, H., Vats, S., Johansson, F., Pedregosa, F., Curry, M. J., Terrel, A. R., Roučka, v., Saboo, A., Fernando, I., Kulal, S., Cimrman, R., & Scopatz, A., 2017. Sympy: symbolic computing in python. *PeerJ Computer Science*, vol. 3, pp. e103.
[7] Gede, G., Peterson, D. L., Nanjangud, A. S., Moore, J. K., & Hubbard, M., 2013. Constrained multibody dynamics with python: From symbolic equation generation to publication. In *Proceedings of the ASME 2013 International Design Engineering Technical Conferences and Computers and Information in Engineering Conference*, Portland, OR. ASME.
[8] Brown, E. L., 2003. *Integrated Strain Actuation In Aircraft With Highly Flexible Composite Wings*. PhD thesis, Massachusetts Institute of Technology.
[9] Hibbeler, R. C., 2015. *Mechanics of materials*. Pearson, Hoboken, NJ.
[10] Han, S. M., Benaroya, H., & Wei, T., 1999. Dynamics of transversely vibrating beans using four engineering theories. *Journal of Sound and Vibration*, vol. 225, pp. 935–988.
[11] Goland, M., 1945. The flutter of a uniform cantilever wing. *Journal of Applied Mechanics*, vol. 12(4), pp. A197–A208.
[12] Fung, Y. C., 1993. *An Introduction to the Theory of Aeroelasticity*. Dover Publications, New York.
[13] Haddadpour, H. & Firouz-Abadi, R. D., 2006. Evaluation of quasi-steady aerodynamic modeling for flutter prediction of aircraft wings in incompressible flow. *Thin-Walled Structures*, vol. 44, pp. 931–936.